Earth and Planetary Science Letters 286 (2009) 576–585

Contents lists available at ScienceDirect

Earth and Planetary Science Letters

journal homepage: www.elsevier.com/locate/epsl

Climate sensitivity to Arctic seaway restriction during the early Paleogene

Christopher D. Roberts [a,*], Allegra N. LeGrande [b], Aradhna K. Tripati [a]

[a] Department of Earth Sciences, University of Cambridge, Cambridge, CB2 3EQ, UK
[b] NASA Goddard Institute of Space Studies and Center for Climate Systems Research, Columbia University, 2880 Broadway, New York, NY 10025, United States

ARTICLE INFO

Article history:
Received 17 March 2009
Received in revised form 25 May 2009
Accepted 23 July 2009
Available online 9 September 2009

Editor: P. DeMenocal

Keywords:
paleoclimate
climate modeling
Paleogene
Arctic Ocean
Azolla
PETM

ABSTRACT

The opening and closing of ocean gateways affects the global distribution of heat, salt, and moisture, potentially driving climatic change on regional to global scales. Between 65 and 45 million years ago (Ma), during the early Paleogene, exchange between the Arctic and global oceans occurred through two narrow and shallow seaways, the Greenland–Norway seaway and the Turgai Strait. Sediments from the Arctic Ocean suggest that, during this interval, the surface ocean was warm, brackish, and episodically enabled the freshwater fern *Azolla* to bloom. The precise mechanisms responsible for the development of these conditions in the Paleogene Arctic remain uncertain. Here we show results from an isotope-enabled, atmosphere-ocean general circulation model, which indicate that Northern Hemisphere climate would have been very sensitive to the degree of oceanic exchange through the Arctic seaways. We also present modelled estimates of seawater and calcite $\delta^{18}O$ for the Paleogene. By restricting these seaways, we simulate freshening of the surface Arctic Ocean to ~6 psu and warming of sea-surface temperatures by 2 °C in the North Atlantic and 5–10 °C in the Labrador Sea. Our results may help explain the occurrence of low-salinity tolerant taxa in the Arctic Ocean during the Eocene and provide a mechanism for enhanced warmth in the north western Atlantic. We propose that the formation of a volcanic land-bridge between Greenland and Europe could have caused increased ocean convection and warming of intermediate waters in the Atlantic. If true, this result is consistent with the theory that bathymetry changes may have caused thermal destabilisation of methane clathrates and supports a tectonic trigger hypothesis for the Paleocene Eocene Thermal Maximum (PETM).

© 2009 Elsevier B.V. All rights reserved.

1. Introduction

Until recently, little was known about climatic and oceanic conditions in the Arctic Ocean during the early Paleogene (65–45 Ma), a 'greenhouse' interval with global temperatures warmer than any other time in the last 65 Ma (Zachos et al., 2001). This period was characterized by high levels of CO_2, warm high latitudes, warm surface-and-deep oceans, and an intensified hydrological cycle (Barron et al., 1989; Lear et al., 2000; Pearson and Palmer, 2000; Tripati and Zachos, 2000; Tripati et al., 2001, 2003; Pagani et al., 2005; Jahren, 2007; Pearson et al., 2007). Following a peak in global temperatures at ~52–50 Ma, there is evidence for declining CO_2, cooling of the high latitudes, and the appearance of sea- and/or glacial-ice in the Northern Hemisphere beginning at 44 Ma (Pearson and Palmer, 2000; Pagani et al., 2005; Tripati et al., 2005, 2008; Moran et al., 2006). In 2004, the first Integrated Ocean Drilling Program expedition to the Lomonosov Ridge (Arctic Coring Expedition — ACEX) recovered ~200 m of sediments from 56–44 Ma (Moran et al., 2006). Studies of these sediments indicated that the Arctic Ocean was a warm, brackish, restricted basin, perhaps similar to the modern Black Sea (Brinkhuis et al., 2006; Pagani et al., 2006; Sluijs et al., 2006; Waddell and Moore, 2008).

1.1. The Azolla event (~48–49 Ma)

A striking feature of the ACEX sediments from ~49–48 Ma is the intermittent appearance of large quantities of microspore clusters from *Azolla* (Brinkhuis et al., 2006), an extant genus of freshwater fern that tolerates salinities up to 5.5 psu (Rai and Rai, 1998). Today, *Azolla* thrives in bodies of standing water including ponds and canals. The *Azolla* variations in Arctic sediments are hypothesized to represent episodic freshening of the surface ocean (Brinkhuis et al., 2006).

Several mechanisms may have been responsible for surface freshening of the Arctic during the middle Eocene. Increased levels of greenhouse gases or changes in the Earth's orbital configuration may have resulted in an enhanced hydrological cycle at the high latitudes. Variations in obliquity would result in changes in the seasonality of insolation at the poles which may have affected the net freshwater balance (precipitation plus run-off, less evaporation) in the Arctic region. Another possibility is that Arctic freshening was controlled by the degree of salt exchange between the Arctic and its adjacent seas (Brinkhuis et al., 2006). By simulating two different tectonic scenarios with a global climate model (GISS ModelE-R), we show that changes in the restriction of the Arctic seaways provide a

* Corresponding author. Tel.: +44 1223 333400; fax: +44 1223 333450.
E-mail address: cdr30@cam.ac.uk (C.D. Roberts).

0012-821X/$ – see front matter © 2009 Elsevier B.V. All rights reserved.
doi:10.1016/j.epsl.2009.07.026

feasible mechanism for driving Arctic freshening during the early Paleogene.

1.2. The Paleocene–Eocene Thermal Maximum (PETM) (55 Ma)

Restriction of the Arctic seaways may also have had implications for the Paleocene–Eocene Thermal Maximum (PETM), another extreme climatic event which was identifiable within the Paleogene ACEX sediments (Pagani et al., 2006; Sluijs et al., 2006, 2008; Stein et al., 2006; Knies et al., 2008; Weller and Stein, 2008). The PETM was a transient (<0.3 Ma) hyperthermal event that occurred 55.5 Myrs ago and was marked by a large (>4‰) negative excursion in marine and terrestrial records of δ^{13}C (Koch et al., 1992; Zachos et al., 2007). The PETM was associated with global warming of 3–8 °C at both high and low latitudes (Zachos et al., 2003, 2006; Tripati and Elderfield, 2004, 2005; Sluijs et al., 2006, 2007a) and warming of 4–5 °C in the deep ocean (Tripati & Elderfield, 2005). Rapid changes in the distribution, diversity, and abundance of marine and terrestrial biota also occur at the PETM (Sluijs et al., 2007b), including evidence for a mass extinction of deep ocean foraminifera (Thomas and Shackleton, 1996). The δ^{13}C excursion, along with evidence for acidification of the deep ocean, has led to the hypothesis that PETM warming was driven by the release of a large mass (>10^{18} g) of isotopically depleted CO_2 or CH_4 into the ocean–atmosphere system (Dickens et al., 1997; Zachos et al., 2005; Panchuk et al., 2008). Suggested sources for this carbon include frozen methane hydrates buried within the sediments on continental margins (e.g., Dickens et al., 1997; Maclennan and Jones, 2006), thermogenic methane derived from contact metamorphism of carbon rich sediments during the intrusion of hot magma (Svenson et al., 2004), extensive burning of terrestrial biomass (Kurtz et al., 2003), and the desiccation of organic matter during the isolation of a large epicontinental seaway (Higgins and Schrag, 2006). The exact mechanisms by which this carbon was released remain controversial, and it is plausible that more than one source of carbon contributed to the spike in records of δ^{13}C. We show that changes in the degree of oceanic exchange between the Arctic and North Atlantic may have led to the destabilization of methane clathrates in the Atlantic.

1.3. Paleogeography

We evaluate climate sensitivity in the early Paleogene to the restriction of the Arctic seaways. Paleogeographic reconstructions for this period show an Arctic Ocean connected to the global oceans by two epicontinental seaways (e.g. Markwick, 2007) (Fig. 1). Connection between the Arctic and Tethys during the Paleogene was through a complex series of straits and epicontinental seas in central Eurasia (Rogl, 1999; Markwick, 2007; Akhmetiev and Beniamovski, 2009). It is likely that the evolution of these seas and gateways during the Cenozoic was highly sensitive to both eustatic and local/tectonic changes in sea level. The Tethys Ocean was connected to the West Siberian Sea via the Turgai Strait, and the West Siberian Sea was connected to the Arctic Ocean through the Kara Sea Strait and a variety of smaller gateways (Akhmetiev and Beniamovski, 2009). Exchange between the Arctic and Tethys occurred most freely during the late Paleocene and early Eocene. By the middle/late Eocene, the West Siberian Sea was isolated from the Arctic Ocean and by the Eocene–Oligocene boundary, the West Siberian Sea had retreated entirely (Rogl, 1999; Akhmetiev and Beniamovski, 2009). For simplicity, we have grouped the central Eurasian seas and straits together and refer to them collectively as the Turgai Strait.

In the Paleogene, exchange between the Arctic and North Atlantic Oceans occurred through the Greenland–Norway Seaway, and until 18 Ma, exchange was limited to the surface ocean (Jakobsson et al., 2007). At ~56 Ma, this seaway may have been restricted by the formation of a transient volcanic land bridge between Greenland and Europe. Uplift was driven by anomalously warm mantle temperatures, crustal thickening, and dynamic support from a mantle plume (Maclennan and Jones, 2006). However, it is unlikely that uplifted crust was a total barrier to surface ocean currents by the middle Eocene (~50 Ma) due to continued sea-floor spreading and thermal subsidence.

Animal migration paths provide evidence for the existence of a land bridge between Asia and North America since at least the late Cretaceous (Averianov and Archibald, 2003). Plate tectonic reconstructions and the separate evolution of marine faunas in the Pacific and Arctic also support the presence of a land bridge between North America and Asia during the Paleogene (Marincovich and Gladenkov, 1999; Markwick, 2007). The opening of the modern Bering Strait is estimated to have occurred 5–7 million years ago at the earliest (Marincovich and Gladenkov, 1999).

The evidence above suggests that, during the Paleogene, exchange between the Arctic and the global oceans most likely occurred through the Greenland–Norway seaway and the Turgai Strait. It is also likely that these two seaways were, at least intermittently, restricted due to tectonic or eustatic changes in sea level. For these reasons, we make these two seaways the focus of our tectonic sensitivity study.

2. Methods

2.1. Model description

We test whether variability in the degree of Arctic seaway restriction is consistent with variability in paleoclimate records for the early Paleogene. Equilibrium climate conditions are simulated for two end-member paleogeographic configurations using the Goddard Institute for

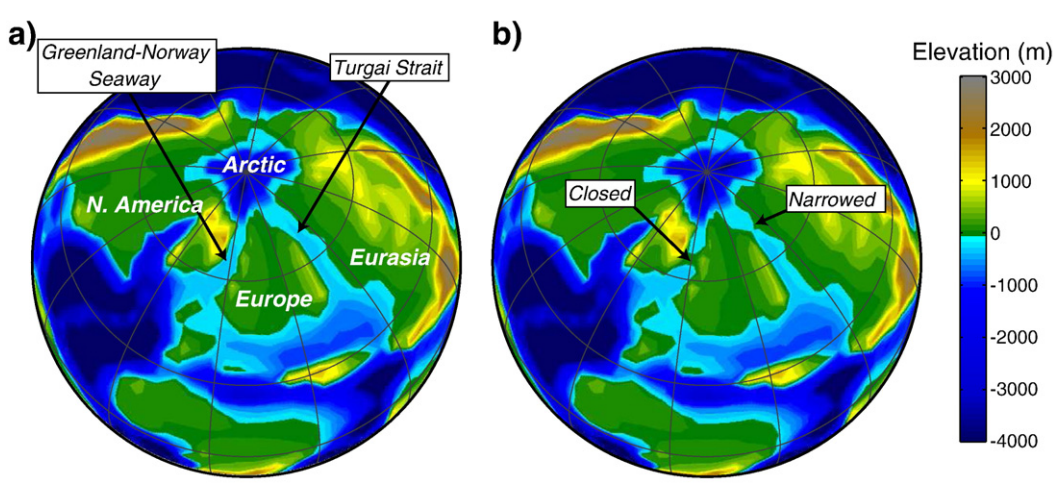

Fig. 1. Bathymetry and topography used in the 'open' (a) and 'closed' (b) Paleogene simulations. Bathymetry and topography data from Bice and Marotzke (2002).

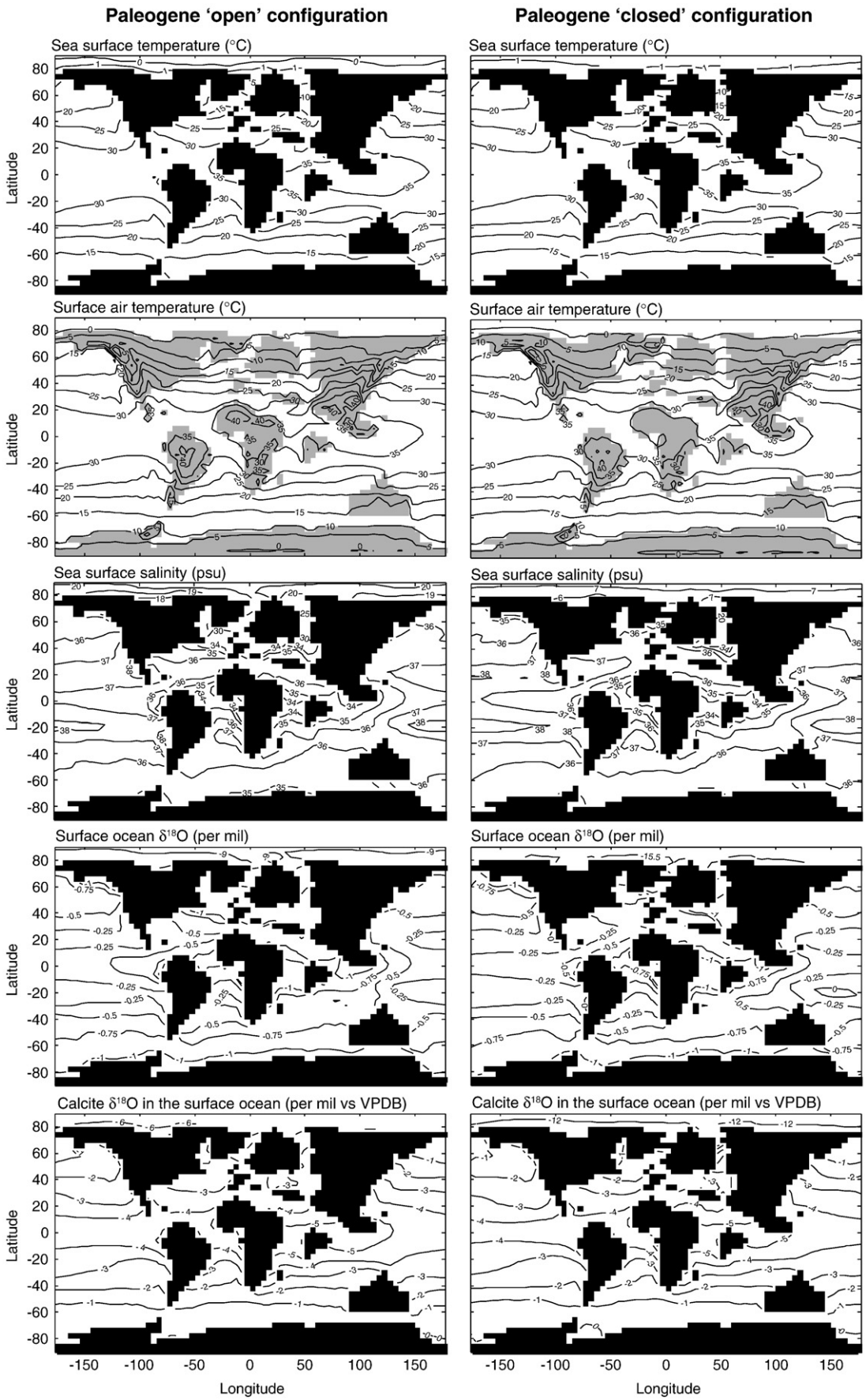

Fig. 2. Annually averaged model fields for sea-surface temperature, surface air temperature, sea-surface salinity, $\delta^{18}O_{seawater}$, and the $\delta^{18}O$ of calcite in equilibrium with surface seawater.

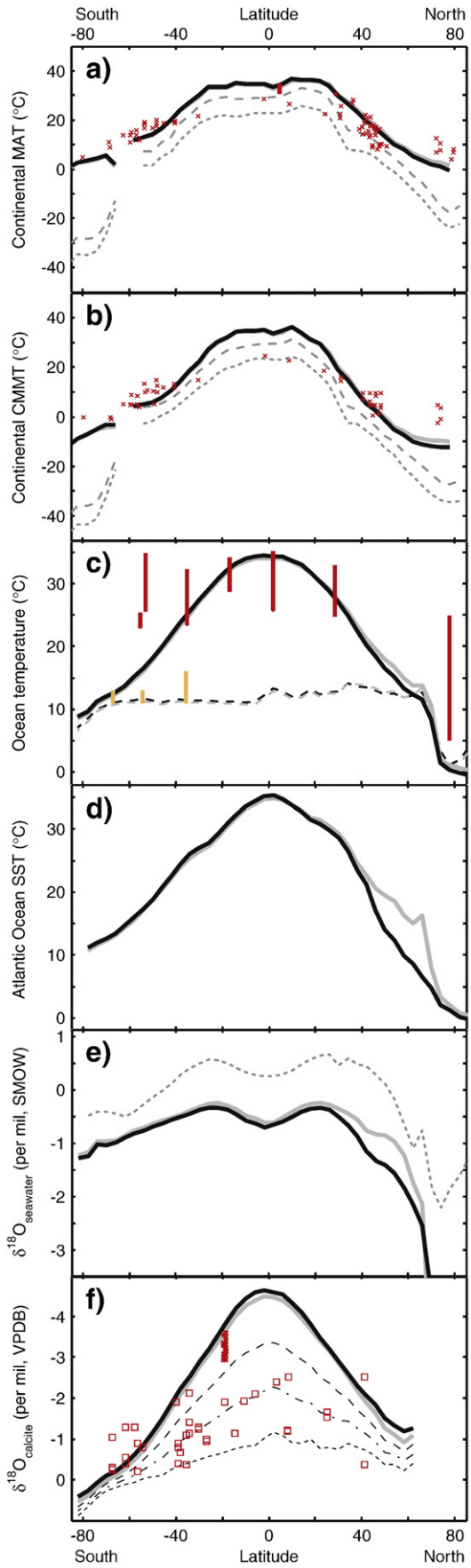

Fig. 3. Zonal averages for selected model fields (thick black lines, 'open' simulation; thick grey lines, 'closed' simulation). Sources for proxy data are listed in Table S1. a) Continental mean annual temperature (MAT). Includes pre-industrial $4\times CO_2$ (dashed line), pre-industrial $1\times CO_2$ (dotted line) and reconstructed values from proxy data (red crosses and red bar). b) Continental cold month mean temperature (CMMT), same legend as (a). c) Simulated sea-surface temperature (SST) compared to proxy estimates of SST (late Paleocene to late Eocene, no PETM values) (red bars) and simulated sea-floor temperature (dashed black line, 'open' simulation; dashed grey line, 'closed' simulation) compared to proxy estimates of sea-floor temperature (orange bars). d) Averaged SST from the Atlantic Ocean. e) Simulated $\delta^{18}O$ composition of seawater, same legend as (a). f) Simulated $\delta^{18}O$ composition of calcite in equilibrium with the surface ocean compared to the $\delta^{18}O$ composition of open ocean foraminifera (red squares) and well-preserved 'glassy' foraminifera (red crosses) from the late Paleocene to early–middle Eocene. The $\delta^{18}O$ composition of calcite estimated assuming a 25% (dashed line), 50% (dash–dot line), and 75% (dotted line) contribution from diagenetic calcite. (For interpretation of the references to colour in this figure legend, the reader is referred to the web version of this article.)

Space Studies (GISS) ModelE-R: an atmosphere–ocean, water isotope-enabled, general circulation model (Schmidt et al., 2007). The atmospheric component of ModelE-R has 20 vertical levels in pressure coordinates (highest level at 0.1 hPa) and a horizontal resolution of $4°\times5°$. This is coupled to a dynamic ocean model with 13 vertical layers and the same horizontal resolution as the atmosphere (Russell et al., 1995). ModelE-R also includes dynamic sea-ice, variable lakes, prescriptive distributions of vegetation and soil types, non-dynamic land ice, and realistic routing of continental precipitation as river run-off. Mass, heat, humidity, salinity, and water isotopes are all traced explicitly. Tracers are advected using a non-diffusive Quadratic Upstream Scheme (QUS) which traces nine sub-grid scale moments in the atmosphere and four moments in the ocean as well as the mean within each box, increasing the effective tracer resolution of the model to $1.3°\times1.6°$ (Schmidt et al., 2006).

Our 'open' simulation allows oceanic exchange with the Arctic through the Greenland–Norway seaway and the Turgai Strait (Fig. 1a), both of which are limited to a depth of 250 m. This configuration represents our 'best guess' scenario for the early Paleogene. Our 'closed' simulation has an Arctic ocean that is much more restricted and has a narrower, shallower (~60 m) Turgai Strait and a closed Greenland–Norway seaway (Fig. 1b). Both the Greenland-Norway Seaway and the Turgai Strait are treated as ocean grid cells in the model. To reduce long integration times, both Paleogene model configurations were initialized using zonally averaged ocean conditions from a 500 year 4× pre-industrial CO_2 run (modern configuration), then integrated for 2000 years of model time with no accelerated 'spin-up' techniques. The $4\times CO_2$ run was initialized from a long pre-industrial control simulation (which was initialized from the Levitus et al. (1994) dataset). Our results should not be sensitive to starting conditions as GISS ModelE-R is not known for supporting multiple equilibria. For the last 100 years of the 2000 year simulations, drift in global mean surface ocean temperature was 0.01 °C/century in the 'closed' configuration and 0.03 °C/century in the 'open' configuration. Temperature drift in the deepest ocean layers was <0.03 °C/century and <0.05 °C/century for the 'closed' and 'open' configurations, respectively. We also compare the last 100 years of the $4\times CO_2$ simulation to the other simulations. After 500 years, temperature drift in the $4\times CO_2$ simulation was 0.25°C/century in the surface ocean and 0.5°C/century in the deep ocean.No adjustment fluxes of energy or moisture were applied.

2.2. Paleogene boundary conditions

Early Paleogene boundary conditions were specified, including elevated greenhouse gases ($4\times CO_2$ and $7\times CH_4$, equivalent to a total of ~4.3× pre-industrial levels of CO_2), altered bathymetry and topography (Bice and Marotzke, 2002), and estimated distribution of vegetation types (Sewall et al., 2000). Mean ocean salinity was adjusted to 35.7 psu, a best estimate derived from consideration of both the volume of water in each component of the hydrosphere and rates of evaporite weathering and deposition (Hay et al., 2006). Global mean

$\delta^{18}O$ and δD of seawater (−0.81‰ and −6.3‰, respectively, relative to the SMOW standard) were adjusted to reflect ice free conditions assuming an average $\delta^{18}O$ composition of −40‰ for modern Antarctic ice, −30‰ for other continental ice, and a deuterium excess of 10‰. Orbital parameters were kept constant (eccentricity = 0.027, obliquity = 23.2°, longitude of perihelion from equinox = 180°) and were estimated for the Paleogene using the calculations of Laskar et al. (2004). Solar luminosity was held constant at the present day value.

3. Results and discussion

3.1. Global patterns

Our early Paleogene simulations are characterised by extreme warmth. Global surface mean annual air temperature (MAT) is 25 °C and pole-equator temperature differences are ~8 °C smaller than those in the pre-industrial control simulation (Schmidt et al., 2007). A pre-industrial configuration with $4\times CO_2$ has a surface MAT of ~20 °C but pole-equator temperature differences are only ~1 °C smaller than those in the pre-industrial control. Incident longwave radiation at the Earth's surface, an indicator of the strength of the greenhouse effect, increases by 34 W/m^2 in the $4\times CO_2$ pre-industrial configuration and 72 W/m^2 in the Paleogene simulations. These comparisons (Figs. 2,3; Table 1) show that half of simulated Paleogene warmth is from greenhouse warming, the remainder is due to changes in other boundary conditions (no ice sheets, paleogeography, albedo, and vegetation) and feedbacks (water vapour, alterations in heat transport, clouds, etc.); this result is roughly consistent with simulations of the early Eocene performed with an uncoupled atmospheric model (Bice, 1997). The advantage of using a coupled model is that the ocean conditions are (1) consistent with the boundary conditions imposed and (2) the ocean can respond to and interact with the atmosphere.

3.2. Model-data comparisons

Our simulated climatologies compare favourably with climate reconstructions for 65–45 Ma (Figs. 2–4), especially with terrestrial data in the mid-latitudes. However, simulated continental MAT (Fig. 3a) and cold month mean temperature (CMMT, Fig. 3b) are too low in the high latitudes and too high in the tropics (though terrestrial

Table 1
Selected climate statistics from the four simulations used in this study.

	Pre-industrial ($1\times CO_2$)	Pre-industrial ($4\times CO_2$)	Paleogene 'open'	Paleogene 'closed'
Global mean values				
Surface air temperature (SAT) (°C)	13.8	18.9	24.9	24.8
Sea-surface temperature (SST) (°C)	18.0	21.8	26.7	26.7
Sea-surface salinity (psu)	35.0	34.8	35.7	35.8
Precipitation/evaporation (mm/day)	3.0	3.2	3.7	3.7
Total cloud cover (%)	59	57	57	57
Specific humidity (g/kg)	8.7	11.7	15.6	15.7
Ground albedo (%)	14.0	13.1	8.4	8.3
Incident LWR[a,b] @surface (W/m^2 − pre-industrial)	0	+34	+72	+72
Reflected SWR[c] @surface (W/m^2 − pre-industrial)	0	−2	−11	−12
Incident SWR[b] @surface (W/m^2 − pre-industrial)	0	−2	−5	−5
Mean values for Arctic Ocean				
Annual SAT (seasonality) (°C)	−16.9 (28 °C)	−9.2 (18 °C)	−1.8 (10 °C)	−0.7 (9 °C)
Annual SST (seasonality) (°C)	−1.7 (0 °C)	−1.4 (1 °C)	0.7 (4 °C)	1.5 (2 °C)
Annual SSS (psu)	31.9	29.6	19.4	6.6
Precipitation (mm/day)	0.6	0.9	1.2	1.2
Evaporation (mm/day)	0.2	0.3	0.3	0.3
Run-off (mm/day)	0.7	0.8	1.8	2.0
P − E + run-off (mm/day)	1.1	1.5	2.7	2.9
Total cloud cover (%)	89	88	86	86
Specific humidity (g/kg)	1.4	2.1	3.3	3.5
Relative humidity (%)	80	85	89	90
Ground albedo (%)	56	49	34	33
Sea-ice coverage (JFD, JJA) (%)	94 (96, 92)	79 (89, 74)	44 (63, 24)	41 (51, 21)
$\delta^{18}O_{sw}$ (permil, vs SMOW)	−1.8	−3.1	−9.2	−15.4
$\delta^{18}O_{calcite}$ (permil, vs VPDB)	2.2	0.9	−5.7	−12.1
$\delta^{18}O_{precip}$ (permil, vs SMOW)	−23	−21	−19	−20
δD_{sw} (permil, vs SMOW)	−14	−24	−55	−102
δD_{precip} (permil, vs SMOW)	−172	−157	−145	−149
Mean values for North Atlantic Ocean				
Annual SAT (seasonality) (°C)	13.7 (5 °C)	15.7 (6 °C)	24.3 (6 °C)	25.9 (6 °C)
Annual SST (seasonality) (°C)	15.9 (3 °C)	17.1 (4 °C)	25.1 (5 °C)	26.9 (5 °C)
Annual SSS (psu)	35.4	34.5	34.9	36.8
Precipitation (mm/day)	2.3	2.0	2.7	3.1
Evaporation (mm/day)	3.4	3.3	4.2	4.8
Run-off (mm/day)	0.4	0.5	0.9	0.9
P − E + run-off (mm/day)	−0.7	−0.8	−0.6	−0.8
Total cloud cover (%)	61	61	56	53
Specific humidity (g/kg)	7.7	7.9	16.6	17.3
Relative humidity (%)	90	90	90	89
$\delta^{18}O_{sw}$ (permil, vs SMOW)	0.4	−0.1	−1.1	−0.4
$\delta^{18}O_{calcite}$ (permil, vs VPDB)	0.4	−0.3	−3.1	−2.7
$\delta^{18}O_{precip}$ (permil, vs SMOW)	−4.6	−4.4	−4.0	−3.5
δD_{sw} (permil, vs SMOW)	2.9	−0.6	−8.5	−3.3
δD_{precip} (permil, vs SMOW)	−27	−26	−22	−17

[a] Long wave (thermal) radiation.
[b] Positive values indicate warming relative to the pre-industrial simulation.
[c] Short wave radiation. Negative values indicate warming relative to the pre-industrial simulation.

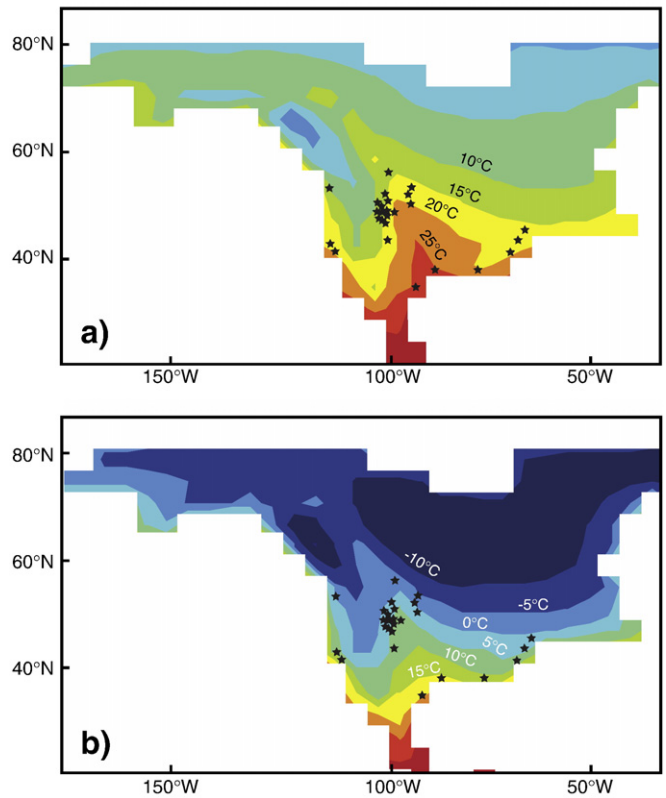

Fig. 4. Mean annual temperature (a) and cold month mean temperature (b) from the 'closed' simulation overlain with localities of Eocene fossil crocodilians (stars; Markwick, 1994).

MAT and CMMT are poorly constrained in the tropics). Both Paleogene simulations produce cool (0–5 °C) Arctic MAT. In contrast, terrestrial data (56–45 Ma) from >78°N indicate above freezing temperatures throughout the polar night and marine proxy-based reconstructions (55–45 Ma) indicate temperatures (with a probable spring-summer bias) of 10–15 °C (Table 2).

Reproducing warmer polar temperatures is possible, but only at the expense of unrealistically high tropical temperatures. This mismatch between proxy and model estimates of high latitude temperatures is a common feature of previous coupled modelling studies (e.g. Huber and Sloan, 2001). Potential causes for mismatches include 1) insufficient sensitivity in coupled models and 2) inaccurate or incomplete model representation of feedback processes that preferentially warm the poles. Previously suggested mechanisms for reducing meridional temperature gradients include cloud-related feedbacks (Sloan et al., 1992; Abbot and Tziperman, 2008), increased ocean mixing driven by tropical cyclones (Korty et al., 2008) and changes to global heat transport (Huber and Sloan, 1999); however, some of these hypotheses (e.g. increased ocean heat transport to high latitudes) have been shown to be unlikely (Huber and Sloan, 2001). The data/model mismatch may also arise from uncertainties associated with the proxy reconstructions.

We also observe a disagreement between Paleogene proxy- and model-based estimates of carbonate oxygen isotope ratios ($\delta^{18}O$) in the surface ocean. At middle and low latitudes, modelled values of equilibrium calcite $\delta^{18}O$ are 1–3‰ lower than foraminiferal values. If we assume our model $\delta^{18}O$ fields are reasonable, this discrepancy may be a result of carbonate ion effects on calcite $\delta^{18}O$ (which our modelled carbonate $\delta^{18}O$ values do not take into account) (Spero et al., 1997; Zeebe, 2001), 'vital effects' or species-specific fractionations (Wefer and Berger, 1991; Bemis et al., 1998), or diagenetic alteration of foraminifera (Pearson et al., 2007) (Fig. 3e). Zeebe (2001) suggested that failure to take into account lower carbonate ion concentrations during past high pCO_2 intervals may bias calcite $\delta^{18}O$ to heavier values (relative to equilibrium) by 0.5–1.0‰, based on the results of culture experiments (Spero et al., 1997). In addition, none of the genera (e.g. *Morozovella*, *Acarinina*) assumed to inhabit the surface layers of the ocean during the Paleogene are extant so it is impossible to know definitively whether the values recorded by their tests are recording true equilibrium values. However, it is well-known from studies of modern planktic foraminifera that vital effects of 0.5 to 1.0‰ can be expressed both within and between species (Bemis et al., 1998), possibly arising from kinetic isotope effects, differences in ambient pH, and/or differences in pH at the site of calcification. Paleocene (57–58 Ma) aragonitic marine molluscs from the Arctic (Tripati and Zachos, 2000; Tripati et al., 2001) are ~5‰ heavier than our simulated equilibrium $\delta^{18}O$ values (Table 3). This difference may arise from vital effects (Wefer and Berger, 1991), molluscs recording non-open ocean conditions, or it could indicate more saline (+10 psu) Arctic conditions (than those simulated) at ~57–58 Ma. Previous studies have also suggested that Paleogene foraminifera recovered from open ocean sites have undergone diagenetic alteration, which would cause them to have much heavier $\delta^{18}O$ values (e.g. Schrag, 1999; Pearson et al., 2001, 2007; Sexton et al., 2006). For example, Pearson et al. (2001) show that exceptionally well-preserved 'glassy' foraminifera

Table 2
Proxy estimates of Arctic temperatures during the early Paleogene.

Reference	Age	Location	Parameter	Value (°C)	Values from model simulations	
					Open config. (°C)	Closed config. (°C)
Basinger (1991)	~45 Ma	Axel Heiberg	MAT[a]	12–15	0.0 °C	3.3 °C
Basinger (1991)	~45 Ma	Axel Heiberg	CMMT[b]	0–4	−16.0 °C	−10.4 °C
Brinkhuis et al. (2006)	~48 to 48.7 Ma	Arctic Ocean	SST[c]	8–14	0.7 °C	1.5 °C
Fricke and Wing (2004)	E. Eocene	Ellesmere Island	MAT	4–8.2	0.0 °C	3.3 °C
Fricke and Wing (2004)	E. Eocene	Axel Heiberg	MAT	9.3	0.0 °C	3.3 °C
Greenwood and Wing (1995)	~45 Ma	Axel Heiberg	MAT	9.3 ± 2.0	0.0 °C	3.3 °C
Greenwood and Wing (1995)	~45 Ma	Axel Heiberg	CMMT	−0.8 ± 3.6	−16.0 °C	−10.4 °C
Jahren (2007)	~45 Ma	Axel Heiberg	MAT	13.2 ± 2	0.0 °C	3.3 °C
Sangiorgi et al. (2008a)	~45 Ma	Arctic Ocean	SST	4–9	0.7 °C	1.5 °C
Sangiorgi et al. (2008b)	46 Ma	Arctic Ocean	SST	8–12	0.7 °C	1.5 °C
Sluijs et al. (2006)	~55 Ma (PETM)	Arctic Ocean	SST	18–23	0.7 °C	1.5 °C
Weller and Stein (2008)	45.0–48.5 Ma	Arctic Ocean	SST	10–25	0.7 °C	1.5 °C
Wolfe (1994)	~45 Ma	Axel Heiberg	MAT	13.7–17.2	0.0 °C	3.3 °C
Wolfe (1994)	~45 Ma	Axel Heiberg	CMMT	3.3–8.6	−16.0 °C	−10.4 °C

[a] MAT = mean annual surface temperature (terrestrial).
[b] CMMT = cold month mean temperature (terrestrial).
[c] SST = sea-surface temperature.

Table 3
Simulated aragonite $\delta^{18}O$ compared with $\delta^{18}O$ of aragonite from Paleocene Arctic molluscs reported by Tripati et al. (2001). All δ^{18} O values are relative to the V-PDB standard.

					Simulated aragonite $\delta^{18}O$ from Ellesmere Island region			
					'Open' simulation		'Closed' simulation	
Mollusc	Habitat	Location	Age (Ma)	$\delta^{18}O \pm 1\sigma$ (‰)	Marine	Terrestrial	Marine	Terrestrial
Dentalium	Marine	Ellesmere Island	57–58	−0.12 ± 0.3	−4.9	−15.4	−11.1	−17.5
Arctica ovata	Estuarine	Ellesmere Island	57–58	−7.94 ± 4.9	−4.9	−15.4	−11.1	−17.5
Corbicula	Estuarine	Ellesmere Island	57–58	−3.92 ± 0.5	−4.9	−15.4	−11.1	−17.5

recovered from hemipelagic clays in Tanzania are as much as 4‰ lighter than foraminifera recovered from an open ocean site that are of a similar age and from a similar latitude. This hypothesis of diagenetic alteration of open ocean samples is supported by scanning electron micrographs of Eocene planktic foraminifera which show evidence for recrystallisation (Sexton et al., 2006).

Analysis of modern crocodilians indicates that the principal climatic control on their distribution is temperature. The critical values for MAT and CMMT—below which crocodilians cannot survive—are 14.2 °C and 5.5 °C, respectively (Markwick, 1998). Simulated MAT and CMMT compare favourably with the distribution of fossil (Eocene age) crocodilians from North America (Fig. 4); however, in both cases model temperatures are too cold north of ~50°N. Cooler model temperatures may in part be explained by uncertainties in the paleoelevation and paleogeography specified as model boundary conditions.

Nevertheless, our simulations reproduce the major features of early Paleogene climate: extreme global warmth, reduced meridional temperature gradients, an enhanced hydrological cycle, and warm oceans.

3.3. Impacts of seaway restriction

Seaway restriction decreases Arctic surface ocean salinity by 12.8 psu and $\delta^{18}O_{sw}$ by 6.2‰. In our 'open' simulation, surface salinities in the Arctic are 18–20 psu, consistent with estimates of 'background' salinity during the Paleogene based on microfossil and palynomorph assemblages, δD isotopes, and the $\delta^{18}O$ of fish bone apatite (Brinkhuis et al., 2006; Pagani et al., 2006; Waddell and Moore, 2008). Mean Arctic surface salinities in our 'closed' simulation are ~7 psu although in some regions salinities are less than 6 psu, close to the maximum reported tolerance of *modern Azolla*. Reduced salinities in the surface Arctic Ocean following restriction of the Arctic seaways is an unsurprising result. However, the fact that Arctic freshening is balanced by a salinity increase in the North Atlantic of 1.8 psu, and not by an increase in salt storage in the deep Arctic Ocean, is a novel finding of this study. This redistribution of salinity occurs because the total mass of salt in the oceans is conserved in our simulations. To preserve this quantity, freshening of the Arctic must be accompanied by increased salt storage somewhere else and our simulations indicate that the majority of this extra salt would end up in the Tethys and North Atlantic. The increased density of North Atlantic surface waters leads to the 'switching on' of a shallow meridional overturning cell in the North Atlantic of 18 Sverdrups (Sv, 10^6 m^3/s) (Fig. 5). The quantitative accuracy of this estimate of ocean overturning depends on the fidelity of the horizontal density gradients in our simulations. However, we believe that increased convection in the Atlantic as a consequence of Arctic seaway restriction is a qualitatively robust result as the simulated changes in circulation are salinity driven. The formation site of this additional convection is centred on the proto-Labrador Sea where SST increases by 5–10 °C, and changes in oceanic heat transport drive Arctic and North Atlantic warming (Fig. 6a–b). Mean annual Arctic SSTs rise by 1 °C and increased poleward heat transport in the North Atlantic (maximum increase of 0.6 Petawatts, 1 PW = 10^{15} Watts) causes localised warming of up to 10 °C (Figs. 3d and 6b). Although inflow from the Atlantic Ocean and Tethys Ocean into the Arctic is reduced by 0.5 and 0.3 Sv respectively—nearly eliminating the minimal oceanic transport of heat into the Arctic present in the 'open' configuration (<0.05 PW)—atmospheric heat transport into the Arctic rises by 0.2 PW; this results in a net increase in northward heat transport and an intensification of the water vapour greenhouse feedback.

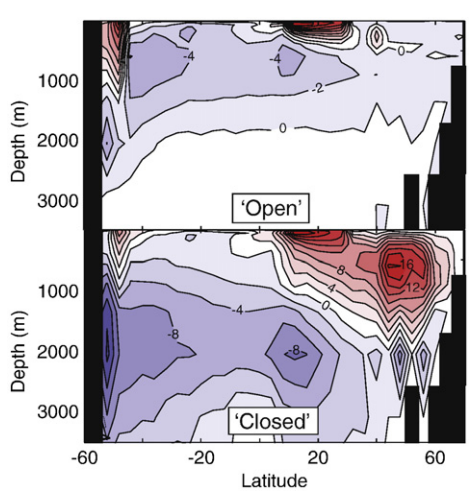

Fig. 5. Meridional overturning stream functions for the Atlantic Ocean in both Paleogene simulations. Red indicates clockwise overturning cells, blue indicates counter-clockwise overturning cells, and the contour spacing is 2 Sverdrups. (For interpretation of the references to colour in this figure legend, the reader is referred to the web version of this article.)

An organic temperature proxy (TEX_{86}) suggests ~3 °C Arctic surface warming at ~48 Ma, synchronous with the disappearance of *Azolla* from Arctic sediments; this warming, and the termination of the *Azolla* blooms, is hypothesised to have been driven by increased oceanic transport of salt and heat into the Arctic (Brinkhuis et al., 2006). However, our simulations indicate that seaway development would have had a minor impact on ocean heat transport. In all our simulations, and in the modern climate system (Wunsch, 2005), poleward oceanic heat transport north of 60°N is minor (<0.1 PW), and the majority of heat transport (>2 PW) is atmospheric. It is unlikely that an ocean current warm and strong enough to cause a temperature anomaly of 3 °C in the Arctic could have existed during the Paleogene. Instead, we speculate that this warming may have been linked to some atmospheric process or feedback (not necessarily heat transport) that is not included in our simulations. Alternatively, changes in TEX_{86} at ~48 Ma may not be reflecting changes in temperature. The mechanism by which these lipids (which are formed throughout the water column) approximate sea-surface conditions is still not known. Turich et al. (2007) suggested that variations in TEX_{86} could be driven by variations in archaeal ecology and/or nutrient concentrations due to rapid shifts in surface water stratification; however, Schouten et al. (2008) dispute these findings.

In both Paleogene simulations, very large vertical density gradients (>5 $kg/m^3/km$, compared to 1.5 $kg/m^3/km$ in the pre-industrial control) inhibit vertical mixing in the Arctic Ocean. These gradients result from surface ocean freshening and would encourage the development of anoxic conditions in the deep Arctic Ocean. The magnitude of these density gradients is so high because salinities in the deep (>1000 m) Arctic Ocean are >10 psu higher than surface

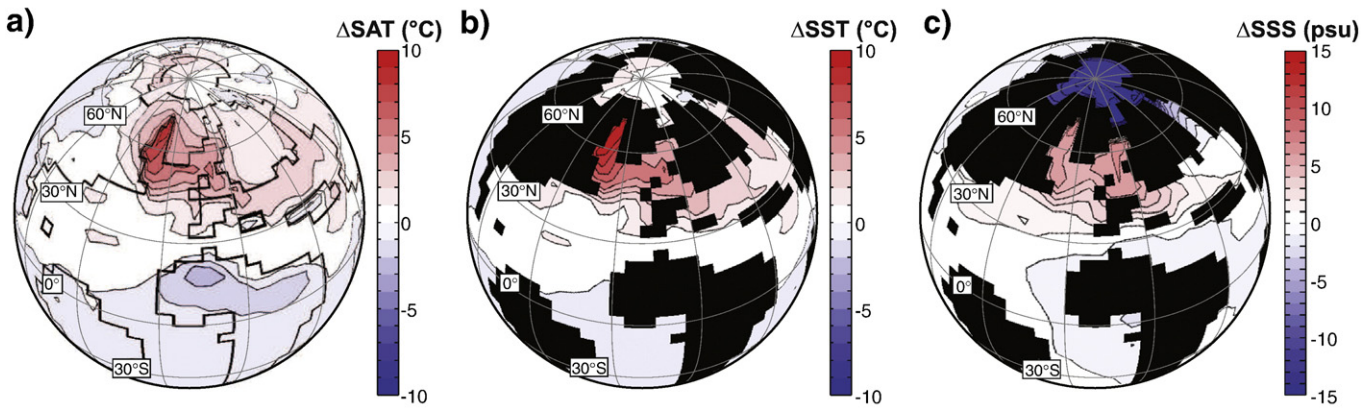

Fig. 6. Difference plots for the Paleogene simulations ('closed'–'open') for (a) surface air temperature, (b) sea-surface temperature, and (c) sea-surface salinity.

values. Our simulations indicate that this salt is slowly escaping to the global oceans at a rate of ~1–2 psu every 500 years; however, surface salinities in the Arctic remain constant. Early Paleogene Arctic sediments are rich in organic carbon, laminated, and contain few benthic fauna (Brinkhuis et al., 2006; Moran et al., 2006; Sluijs et al., 2006; Knies et al., 2008; Onodera et al., 2008; O'Regan et al., 2008; Sluijs et al., 2008; Stickley et al., 2008; Waddell and Moore, 2008; Weller and Stein, 2008), conditions consistent with our simulations.

Simulated Arctic warming, following seaway restriction, is associated with a slight intensification of the hydrological cycle, and a corresponding increase in net freshwater balance into the Arctic basin. Reduced inter-basin exchange of salt and the intensified Arctic hydrological cycle ultimately drive the redistribution of salinity between the Arctic and Atlantic Oceans (Fig. 6c).

Our simulations can also be interpreted within the context of the PETM. The establishment of a warm and salty intermediate water mass in our 'closed' simulation warms intermediate depths (~1700 m) throughout the Atlantic by 1.0–2.5 °C (Fig. 7). Previous studies have noted the synchronicity of the PETM and of the North Atlantic Igneous Province (Svenson et al., 2004; Maclennan and Jones 2006; Storey et al., 2007), and results from an uncoupled ocean model indicate that restricting exchange between the Arctic and North Atlantic would change ocean circulation and cause deep ocean warming (Bice and Marotzke, 2002). The results from our 'closed' simulation indicate that the formation of a Greenland–Europe land bridge would have caused warming of surface and intermediate waters in the Atlantic, potentially triggering the destabilisation and sudden release of frozen methane clathrates from ocean sediments. This result is consistent with evidence from New Jersey (USA) which indicates surface warming of 3–4 °C, several thousand years before the onset of the PETM (Sluijs et al., 2007a,b). The initial release of methane hydrates in the Atlantic and subsequent global warming may have then acted as a catalyst for further re-organisation of global ocean circulation (Tripati and Elderfield, 2005). The consequences for clathrate stability due to this pattern of ocean warming are the subject of ongoing study.

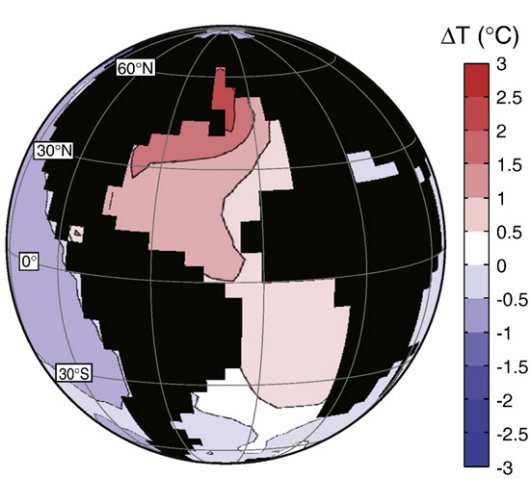

Fig. 7. Difference in ocean temperature ('closed'–'open') at a depth of ~1700 m.

4. Conclusions

We suggest that some degree of seaway restriction was a necessary precondition for the appearance of *Azolla* in the Arctic Ocean. This freshening paired with another mechanism, possibly an astronomically-paced forcing or changes in greenhouse gases, may explain the intermittent appearance of *Azolla* in the ACEX sediments. Arctic surface salinities from our 'open' simulation are consistent with brackish 'background' values reconstructed from a range of proxies (Brinkhuis et al., 2006; Pagani et al., 2006; Waddell and Moore, 2008); in our 'closed' simulation, an extreme case of Arctic restriction, surface salinities approach within 1 psu of the maximum reported values tolerated by *Azolla*.

Our sensitivity study also supports a hypothesis for a tectonic trigger of the Paleocene–Eocene Thermal Maximum (PETM). Restriction of the Arctic seaways results in warming of North Atlantic intermediate waters by 1.0–2.5 °C which could have destabilised methane hydrates on continental margins.

In the study of 'greenhouse' climates, an important question remains unanswered: what mechanisms were responsible for polar warmth and the severe reduction in meridional temperature gradients during the early Paleogene? Changing the degree of oceanic exchange through the Arctic seaways does not explain this pattern. Future climate model sensitivity studies need to focus on identifying novel processes that preferentially warm the high latitudes and impede freezing during the polar night or reduce tropical climate sensitivity to greenhouse gases.

Acknowledgements

We thank NASA GISS for institutional support and acknowledge financial support from the Natural Environment Research Council (studentship NER/S/A/2006/14070 and fellowship NE/D009049/1), the National Science Foundation (ATM 0753660), and Magdalene College. We thank G. Schmidt for helpful discussions and K. Bice and J. Sewall for providing us with gridded data for the boundary conditions. Constructive reviews from four anonymous reviewers improved this manuscript.

Appendix A. Supplementary data

Supplementary data associated with this article can be found, in the online version, at doi:10.1016/j.epsl.2009.07.026.

References

Abbot, D.S., Tziperman, E., 2008. A high-latitude convective cloud feedback and equable climates. Q. J. R. Meteorol. Soc. 134, 165–185.

Akhmetiev, M.A., Beniamovski, V.N., 2009. Paleogene floral assemblages around epicontinental seas and straits in Northern Central Eurasia: proxies for climatic and paleogeographic evolution. Geol. Acta 7, 297–309.

Averianov, A.O., Archibald, J.D., 2003. Mammals from the Upper Cretaceous Aitym Formation, Kyzylkum Desert, Uzbekistan. Cretac. Res. 24, 171–191.

Barron, E.J., Hay, W.W., Thompson, S., 1989. The hydrologic-cycle — a major variable during Earth history. Glob. Planet. Change 75, 157–174.

Basinger, J.F., 1991. The fossil forests of the Buchanan Lake Formation (early Tertiary), Axel Heiberg Island, Canadian Arctic Archipelago: preliminary floristics and paleoclimate. In: Christie, R.L., McMillan, N.J. (Eds.), Tertiary Fossil Forests of the Geodetic Hills, Axel Heiberg Island, Arctic Archipelago. Geological Survey of Canada, Ottawa, pp. 39–65.

Bemis, B.E., Spero, H.J., Bijma, J., Lea, D.W., 1998. Reevaluation of the oxygen isotopic composition of planktonic foraminifera: experimental results and revised paleotemperature equations. Paleoceanography 13, 150–160.

Bice, K.L., 1997. An Investigation of Early Eocene Deep Water Warmth Using Uncoupled Atmosphere and Ocean General Circulation Models: Model Sensitivity to Geography, Initial Temperatures, Atmospheric Forcing And Continental Runoff. PhD Thesis, Dept. of Geosci., Pa. State Univ., 363 pp.

Bice, K.L., Marotzke, J., 2002. Could changing ocean circulation have destabilized methane hydrate at the Paleocene/Eocene boundary? Paleoceanography 17, 1–12.

Brinkhuis, H., Schouten, S., Collinson, M.E., Sluijs, A., Sinninghe Damste, J.S., Dickens, G.R., Huber, M., Cronin, T.M., Onodera, J., Takahashi, K., Bujak, J.P., Stein, R., van der Burgh, J., Eldrett, J.S., Harding, I.C., Lotter, A.F., Sangiorgi, F., van Konijnenburg-van Cittert, H., de Leeuw, J.W., Matthiessen, J., Backman, J., Moran, K., Expedition 302 Scientists, 2006. Episodic fresh surface waters in the Eocene Arctic Ocean. Nature 441, 606–609.

Dickens, G.R., Castillo, M.M., Walker, J.C.G., 1997. A blast of gas in the latest Paleocene: Simulating first-order effects of massive dissociation of oceanic methane hydrate. Geology 25, 259–262.

Fricke, H.C., Wing, S.L., 2004. Oxygen isotope and paleobotanical estimates of temperature and $d^{18}O$-latitude gradients over North America during the early Eocene. Am. J. Sci. 304, 612–635.

Greenwood, D.R., Wing, S.L., 1995. Eocene continental climates and latitudinal temperature gradients. Geology 23 (11), 1044–1048.

Hay, W.W., Migdisov, A., Balukhovsky, A.N., Wold, C.N., Flogel, S., Soding, E., 2006. Evaporites and the salinity of the ocean during the Phanerozoic: implications for climate, ocean circulation and life. Palaeogeogr. Palaeoclimatol. Palaeoecol. 240, 3–46.

Higgins, J.A., Schrag, D.P., 2006. Beyond methane: towards a theory for the Paleocene–Eocene thermal maximum. Earth Planet. Sci. Lett. 245, 523–537.

Huber, M., Sloan, L.C., 1999. Warm climate transitions: a general circulation modeling study of the late Paleocene thermal maximum (~56 Ma). J. Geophys. Res. 104, 16633–16655.

Huber, M., Sloan, L.C., 2001. Heat transport, deep waters, and thermal gradients: coupled simulation of an Eocene greenhouse climate. Geophys. Res. Lett. 28, 3481–3484.

Jahren, A.H., 2007. The Arctic forest of the middle Eocene. Annu. Rev. Earth Planet. Sci. 35, 509–540.

Jakobsson, M., Backman, J., Rudeks, B., Nycander, J., Frank, M., Mayer, L., Jokat, W., Sangiorgi, F., O'Regan, M., Brinkhuis, H., King, J., Moran, K., 2007. The early Miocene onset of a ventilated circulation regime in the Arctic Ocean. Nature 447, 986–990.

Koch, P.L., Zachos, J.C., Gingerich, P.D., 1992. Correlation between isotope records in marine and continental carbon reservoirs near the Paleocene/Eocene boundary. Nature 358, 319–322.

Korty, R.L., Emanuel, K.A., Scott, J.R., 2008. Tropical cyclone-induced upper-ocean mixing and climate: application to equable climates. J. Climate 21, 638–654.

Knies, J., Mann, U., Popp, B.N., Stein, R., Brumsack, H., 2008. Surface water productivity and paleoceanographic implications in the Cenozoic Arctic Ocean. Paleoceanography 23. doi:10.1029/2007PA001455.

Kurtz, A.C., Kump, L.R., Arthur, M.A., Zachos, J.C., Paytan, A., 2003. Early Cenozoic decoupling of the global carbon and sulfur cycles. Paleoceanography 18. doi:10.1029/2003PA000908.

Laskar, J., Robutel, P., Joutel, F., Gastineau, M., Correia, A.C.M., Levrard, B., 2004. A long-term numerical solution for the insolation quantities of the Earth. Astron. Astrophys. 428, 261–285.

Lear, C.H., Elderfield, H., Wilson, P.A., 2000. Cenozoic deep-sea temperatures and global ice volumes from Mg/Ca in benthic foraminiferal calcite. Science 287, 269–272.

Levitus, S., Burgett, R., Boyer, T.P., 1994. World Ocean Atlas 1994. U.S. Department of Commerce, Washington D.C.. Tech. rep.

Maclennan, J., Jones, S.M., 2006. Regional uplift, gas hydrate dissociation and the origins of the Paleocene–Eocene thermal maximum. Earth Planet. Sci. Lett. 245, 65–80.

Marincovich, J., Gladenkov, A.Y., 1999. Evidence for an early opening of the Bering Strait. Nature 397, 149–151.

Markwick, P.J., 1994. "Equability," continentality, and Tertiary "climate": the crocodilian perspective. Geology 22, 613–616.

Markwick, P.J., 1998. Fossil crocodilians as indicators of late Cretaceous and Cenozoic climates: implications for using palaeontological data in reconstructing palaeoclimate. Palaeogeogr. Palaeoclimatol. Palaeoecol. 137, 205–271.

Markwick, P.J., 2007. The palaeogeographic and palaeoclimatic significance of climate proxies for data-model comparisons. In: Williams, M., Haywood, A.M., Gregory, F.J., Schmidt, D.N. (Eds.), Deep-time Perspective on Climate Change: Marrying the Signal from Computer Models and Biological Proxies, The Micropalaeontological Society, Special Publications, The Geological Society, London, pp. 251–312.

Moran, K., Backman, J., Brinkhuis, H., Clemens, S.C., Cronin, T., Dickens, G.R., Eynaud, F., Gattacceca, J., Jakobsson, M., Jordan, R.W., Kaminski, M., King, J., Koc, N., Krylov, A., Martinez, N., Matthiessen, J., McInroy, D., Moore, T.C., Onodera, J., O ' Regan, M., Pälike, H., Rea, B., Rio, D., Sakamoto, T., Smith, D.C., Stein, R., St John, K., Suto, I., Suzuki, N., Takahashi, K., Watanabe, M., Yamamoto, M., Farrell, M., Frank, M., Kubik, P., Jokat, W., Kristoffersen, Y., 2006. The Cenozoic palaeoenvironment of the Arctic Ocean. Nature 441, 601–605.

O'Regan, A., Moran, K., Backman, J., Jakobsson, M., Sangiorgi, F., Brinkhuis, H., Pockalny, R., Skelton, A., Stickley, C., Koc, N., Brumsack, H., Willard, D., 2008. Mid-Cenozoic tectonic and paleoenvironmental setting of the central Arctic ocean. Paleoceanography 23. doi:10.1029/2007PA001559.

Onodera, J., Takahashi, K., Jordan, R.W., 2008. Eocene silicoflagellate and ebridian paleoceanography in the central Arctic ocean. Paleoceanography 23. doi:10.1029/2007PA001474.

Pagani, M., Zachos, J.C, Freeman, K.H., Tipple, B., Bohaty, S., 2005. Marked decline in atmospheric carbon dioxide concentrations during the Paleogene. Science 309, 600–603.

Pagani, M., Pedentchouck, N., Huber, M., Sluijs, A., Schouten, S., Brinkhuis, H., Sinninghe Damste, J.S., Dickens, G., Expedition 302 Scientists, 2006. Arctic hydrology during global warming at the Palaeocene/Eocene thermal maximum. Nature 443, 671–675.

Panchuk, K., Ridgwell, A., Kump, L.R., 2008. Sedimentary response to Paleocene–Eocene thermal maximum carbon release: a model-data comparison. Geology 36, 315–318.

Pearson, P.N., Palmer, M.R., 2000. Atmospheric carbon dioxide concentrations over the past 60 million years. Nature 406, 695–699.

Pearson, P.N., Ditchfield, P.W., Singano, J., Harcourt-Brown, K.G., Nicholas, C.J., Olsson, R.K., Shackleton, N.J., Hall, M.A., 2001. Warm tropical sea surface temperatures in the late Cretaceous and Eocene epochs. Nature 413, 481–487.

Pearson, P.N., van Dongen, B.E., Nicholas, C.J., Pancost, R.D., Schouten, S., Singano, J.M., Wade, B.S., 2007. Stable warm tropical climate through the Eocene Epoch. Geology 35, 211–214.

Rai, V., Rai, A., 1998. Growth behaviour of *Azolla pinnata* at various salinity levels and induction of high salt tolerance. Plant Soil 206, 175–178.

Rogl, F., 1999. Mediterranean and Paratethys. Facts and hypotheses of an Oligocene to Miocene paleogeography (short overview). Geol. Carpath. 50, 339–349.

Russell, G.L., Miller, J.R., Rind, D., 1995. A coupled atmosphere–ocean model for transient climate change studies. Atmosphere–Ocean 33, 683–730.

Sangiorgi, F., Brumsack, H., Willard, D.A., Schouten, S., Stickley, C.E., O'Regan, M., Reichart, G., Sinninghe Damste, J.S., Brinkhuis, H., 2008a. A 26 million year gap in the central Arctic record at the greenhouse-icehouse transition: looking for clues. Paleoceanography 23. doi:10.1029/2007PA001477.

Sangiorgi, F., van Soelen, E.E., Spofforth, D.J.A., Palike, H., Stickley, C.E., St. John, K., Koc, N., Schouten, S., Sinninghe Damste, J.S, Brinkhuis, H., 2008b. Cyclicity in the middle Eocene central Arctic ocean sediment record: orbital forcing and environmental response. Paleoceanography 23. doi:10.1029/2007PA001487.

Schmidt, G.A., Ruedy, R., Hansen, J.E., Aleinov, I., Bell, N., Bauer, M., Bauer, S., Cairns, B., Canuto, V., Cheng, Y., Del Genio, A., Faluvegi, G., Friend, A.D., Hall, T.M., Hu, Y.Y., Kelley, M., Kiang, N.Y., Koch, D., Lacis, A.A., Lerner, J., Lo, K.K., Miller, R.L., Nazarenko, L., Oinas, V., Perlwitz, J., Perlwitz, J., Rind, D., Romanou, A., Russell, G.L., Sato, M., Shindell, D.T., Stone, P.H., Sun, S., Tausnev, N., Thresher, D., Yao, M.S., 2006. Present-day atmospheric simulations using GISS ModelE: comparison to in situ, satellite, and reanalysis data. J. Climate 19, 153–192.

Schmidt, G.A., LeGrande, A.N., Hoffmann, G., 2007. Water isotope expressions of intrinsic and forced variability in a coupled ocean–atmosphere model. J. Geophys. Res.-Atmos. 112, 1–18.

Schouten, S., van der Meer, M.T.J., Hopmans, E.C., Sinninghe Damste, J.S., 2008. Comment on "Lipids of marine Archaea: patterns and provenance in the water column and sediments" by Turich et al. (2007). Geochim. Cosmochim. Acta 72, 5342–5346.

Schrag, D.P., 1999. Effects of diagenesis on the isotopic record of late Paleogene tropical sea surface temperatures. Chem. Geol. 161, 215–224.

Sewall, J.O., Sloan, L.C., Huber, M., Wing, W., 2000. Climate sensitivity to changes in land surface characteristics. Glob. Planet. Change 26, 445–465.

Sexton, P.F., Wilson, P.A., Pearson, P.N., 2006. Microstructural and geochemical perspectives on planktic foraminiferal preservation: "glassy" versus "frosty". Geochem. Geophys. Geosyst. 7. doi:10.1029/2006GC001291.

Sloan, L.C., Walker, J.C.G., Moore Jr., T.C., Rea, D.K., Zachos, J.C., 1992. Possible methane-induced polar warming in the early Eocene. Nature 357, 320–322.

Sluijs, A., Schouten, S., Pagani, M., Woltering, M., Brinkhuis, H., Damste, J.S.S., Dickens, G.R., Huber, M., Reichart, G.J., Stein, R., Matthiessen, J., Lourens, L.J., Pedentchouk, N., Backman, J., Moran, K., Expedition 302 Scientists, 2006. Subtropical arctic ocean temperatures during the Palaeocene/Eocene thermal maximum. Nature 441, 610–613.

Sluijs, A., Brinkhuis, H., Schouten, S., Bohaty, S.M., John, C.M., Zachos, J.C., Reichart, G., Sinninghe Damste, J.S., Crouch, E.M., Dickens, G.R., 2007a. Environmental precursors to rapid light carbon injection at the Paleocene/Eocene boundary. Nature 450, 1218–1221.

Sluijs, A., Bowen, G.J, Brinkhuis, H., Lourens, L.J., Thomas, E., 2007b. The Paleocene–Eocene thermal maximum super greenhouse: biotic and geochemical signatures, age models

and mechanisms of global change. In: Williams, M., Haywood, A.M., Gregory, F.J., Schmidt, D.N. (Eds.), Deep-time Perspective on Climate Change: Marrying the Signal from Computer Models and Biological Proxies, The Micropalaeontological Society, Special Publications, The Geological Society, London, pp. 323–349.

Sluijs, A., Röhl, U., Schouten, S., Brumsack, H., Sangiorgi, F., Sinninghe Damsté, J.S., Brinkhuis, H., 2008. Arctic late Paleogene–early Eocene paleoenvironments with special emphasis on the Paleocene–Eocene thermal maximum (Lomonosov Ridge, Integrated Ocean Drilling Program Expedition 302). Paleoceanography 23. doi:10.1029/2007PA001495.

Spero, H.J., Bijma, J., Lea, D.W., Bemis, B.E., 1997. Effect of seawater carbonate concentration on foraminiferal carbon and oxygen isotopes. Nature 390, 497–500.

Stein, R., Boucsein, B., Meyer, H., 2006. Anoxia and high primary production in the Paleogene central Arctic Ocean: first detailed records from Lomonosov Ridge. Geophys. Res. Lett. 33. doi:10.1029/2006GL026776.

Stickley, C.E., Koc, N., Brumsack, H., Jordan, R.W., Suto, I., 2008. A siliceous microfossil view of middle Eocene Arctic paleoenvironments: a window of biosilica production and preservation. Paleoceanography 23. doi:10.1029/2007PA001485.

Storey, M., Duncan, R.A., Swisher, C.C., 2007. Paleocene–Eocene thermal maximum and the opening of the northeast Atlantic. Science 316, 587–589.

Svenson, H., Planke, S., Malthe-Sorenssen, A., Jamtveit, B., Myklebust, R., Rasmussen Eidem, T., Rey, S.S., 2004. Release of methane from a volcanic basin as a mechanism for initial Eocene global warming. Nature 429, 542–545.

Thomas, E., Shackleton, N.J., 1996. The Paleocene–Eocene benthic foraminiferal extinction and stable isotope anomalies. In: Knox, R.W.O.B., Corfield, R.M., Dunay, R.E. (Eds.), Correlation of the Early Paleogene in Northwestern Europe. Geological Society London Special Publication 101. Geological Society of London, pp. 401–441.

Tripati, A.K., Zachos, J., 2000. Paleocene and Eocene coastal temperatures. GFF 122, 171–172.

Tripati, A.K., Elderfield, H., 2004. Abrupt hydrographic changes in the equatorial Pacific and subtropical Atlantic from foraminiferal Mg/Ca indicate greenhouse origin for the thermal maximum at the Paleocene–Eocene boundary. Geochem. Geophys. Geosyst. 5 (2), 1–11.

Tripati, A.K., Elderfield, H., 2005. Deep-sea temperature and circulation changes at the Paleocene–Eocene thermal maximum. Science 308, 1894–1898.

Tripati, A.K., Zachos, J., Marincovich Jr., L., Bice, K., 2001. Late Paleocene Arctic coastal climate inferred from molluscan stable and radiogenic isotope ratios. Palaeogeogr. Palaeoclimatol. Palaeoecol. 170, 101–113.

Tripati, A.K., Delaney, M.L., Zachos, J.C., Anderson, L.D., Kelly, D.C., Elderfield, H., 2003. Tropical sea-surface temperature reconstruction for the early Paleogene using Mg/Ca ratios of planktonic foraminifera. Paleoceanography 18. doi:10.1029/2003PA000937.

Tripati, A.K., Backman, J., Elderfield, H., Ferretti, P., 2005. Eocene bipolar glaciation associated with global carbon cycle changes. Nature 436, 341–346.

Tripati, A.K., Eagle, R.A., Morton, A., Dowdeswell, J.A., Atkinson, K.L., Bahe, Y., Dawber, C.F., Khadun, E., Shaw, R.M.H., Shorttle, O., Thanabalasundaram, L., 2008. Evidence for glaciation in the Northern Hemisphere back to 44 Ma from ice-rafted debris in the Greenland Sea. Earth Planet. Sc. Lett. 265, 112–122.

Turich, C., Freeman, K.H., Bruns, M.A., Conte, M., Jones, A.D., Wakeham, S.G., 2007. Lipids of marine Archaea: patterns and provenance in the water-column and sediments. Geochim. Cosmochim. Acta 71, 3272–3291.

Waddell, L.M., Moore, T.C., 2008. Salinity of the Eocene Arctic Ocean from oxygen isotope analysis of fish bone carbonate. Paleoceanography 23, 1–14.

Wefer, G., Berger, W.H., 1991. Isotope paleontology: growth and composition of extant calcareous species. Mar. Geol. 100, 207–248.

Weller, P., Stein, R., 2008. Paleogene biomarker records from the central Arctic Ocean (Integrated Ocean Drilling Program Expedition 302): organic carbon sources, anoxia, and sea surface temperature. Paleoceanography 23. doi:10.1029/2007PA001472.

Wolfe, J.A., 1994. Alaskan Palaeogene climates as inferred from the CLAMP database. In: Boulter, M.C., Fisher, H.C. (Eds.), Cenozoic Plants and Climates of the Arctic. Springer Verlag, pp. 223–237.

Wunsch, C., 2005. The total meridional heat flux and its oceanic and atmospheric partition. J. Climate 18 (21), 4374–4380.

Zachos, J., Pagani, M., Sloan, L., Thomas, E., Billups, K., 2001. Trends, rhythms, and aberrations in global climate 65 Ma to present. Science 292, 686–693.

Zachos, J.C., Wara, M.W., Bohaty, S., Delaney, M.L., Petrizzo, M.R., Brill, M., Bralower, T.J., Premoli-Silva, I., 2003. A transient rise in tropical sea surface temperatures during the Paleocene–Eocene thermal maximum. Science 302, 1551–1554.

Zachos, J.C., Rohl, U., Schellenberg, S.A., Sluijs, A., Hodell, D.A., Kelly, D.C., Thomas, E., Nicolo, M., Raffi, I., Lourens, L.J., McCarren, H., Kroon, D., 2005. Rapid acidification of the ocean during the Paleocene–Eocene thermal maximum. Science 308, 1611–1615.

Zachos, J.C., Shouten, S., Sluijs, A., Quattlebaum, T., Brinkhuis, H., Gibbs, S.J., Bralower, T. J., 2006. Extreme warming of mid-latitude coastal ocean during the Paleocene–Eocene thermal maximum: inferences from TEX_{86} and isotope data. Geology 34, 737–740.

Zachos, J.C., Bohaty, S.M., John, C.M., McCarren, H., Kelly, D.C., Nielsen, T., 2007. The Paleocene–Eocene carbon isotope excursion: constraints from individual shell planktonic foraminifer records. Phil. Trans. R. Soc. 365, 1829–1842.

Zeebe, R., 2001. Seawater pH and isotopic paleotemperatures of Cretaceous oceans. Palaeogeogr. Palaeoclimatol. Palaeoecol. 170, 49–57.